Characterization of Micron-Sized Periodic Structures in Multicomponent Polymer Blends by Ultra-Small-Angle Neutron Scattering and Optical Microscopy

Nisita S. Wanakule,[†] Alisyn J. Nedoma,[†] Megan L. Robertson,[†] Zhuangxi Fang,[‡] Andrew Jackson,[§,||] Bruce A. Garetz,[⊥] and Nitash P. Balsara*[,†,#,×]

Department of Chemical Engineering, University of California, Berkeley, California 94720; Othmer-Jacobs Department of Chemical & Biological Engineering, Polytechnic University, Brooklyn, New York 11201; NIST Center for Neutron Research, National Institute of Standards and Technology, Gaithersburg, Maryland 20899; Department of Materials Science and Engineering, University of Maryland, College Park, Maryland 20742; Department of Chemical and Biological Sciences, Polytechnic University, Brooklyn, New York 11201; Environmental and Energy Technologies Division, Lawrence Berkeley National Laboratory, Berkeley, California 94720; and Materials Sciences Division, Lawrence Berkeley National Laboratory, Berkeley, California 94720

Received August 27, 2007; Revised Manuscript Received October 18, 2007

ABSTRACT: The thermodynamic properties of a multicomponent blend containing nearly equal volume fractions of two homopolymers, a saturated polybutadiene with 89% 1,2-addition (component A) and polyisobutylene (component B), and 1 vol % of a diblock copolymer was studied by a combination of ultra-small-angle neutron scattering (USANS) and optical microscopy. The A−C diblock copolymer, which serves as a surfactant, has an A block that is chemically identical to the A homopolymer and a C block that is a saturated polybutadiene with 62% 1,2-addition. The C block exhibits attractive interactions with component B and repulsive interactions with component A. At temperatures between room temperature and 45 °C, USANS results indicated that this blend self-assembles into a microemulsion with periodic length scales in the 0.2−4 μm range. The USANS data were in excellent agreement with the Teubner−Strey equation for scattering from microemulsions. Optical microscopy studies revealed the presence of bicontinuous microemulsions with length scales that were commensurate with those obtained by USANS.

Introduction

Most polymers are sparingly soluble in each other, and thus mixtures of different polymers naturally separate into distinct phases. Controlling the morphology of phase-separated polymer blends is a subject of long-standing technological and fundamental interest.[1−12] In many cases, block copolymers are used as surfactants for stabilizing the interface between two immiscible homopolymers that we label A and B. Strategies for interfacial stabilization depend on the curvature of the interface, which, in turn, depends on the relative volume fractions of the homopolymers.[13] The present paper is focused on mixtures containing equal (or nearly so) volume fractions of the A and B homopolymers and diblock copolymers that are symmetric in composition. In most cases, mixtures of homopolymers and block copolymers form disorganized, macrophase-separated morphologies. There exists, however, a range of thermodynamic conditions (concentration, temperature, and pressure) where these systems self-organize into periodic structures such as lamellae, droplet microemulsions, and bicontinuous microemulsions.[1−4,14] In the limit of large block copolymer concentration (typically above 50 vol %), lamellar phases are obtained.[4] As the block copolymer concentration is decreased, the lamellar phases first transform into bicontinuous microemulsions and ultimately give way to macrophase-separated states.[3,14,15] The minimum surfactant volume fraction needed to form a single-phase system (e.g., lamellae and microemulsions), $\varphi_{s,min}$, is a measure of the efficacy of the surfactant. Bicontinuous microemulsions are usually obtained in a narrow window in the vicinity of $\varphi_{s,min}$. It is clear that the extent to which a given lamellar phase can be swollen by homopolymers is intimately related to $\varphi_{s,min}$. The purpose of the paper is to explore the morphology and thermodynamics of a polymer blend in the vicinity of $\varphi_{s,min}$.

The traditional approach of organizing mixtures of A and B homopolymers is to use block or graft copolymers of A and B as the surfactant. In these systems with volume fractions of A and B approximately equal, organized structures require at least 9 vol % of the A−B surfactants, i.e., $\varphi_{s,min} = 0.09$.[3,16−18] An alternative method is to mimic the design of nonionic surfactants for oil/water systems.[19−23] This approach, which has been established in a series of publications,[14,24−32] utilizes an A−C diblock copolymer as the surfactant, where the C block exhibits attractive interactions with the B homopolymer and repulsive interactions with the A homopolymer. In ref 31, it was shown that $\varphi_{s,min}$ for a particular A/B/A−C blend can be as low as 0.01. This conclusion was based on small-angle neutron scattering (SANS) experiments where the coherent scattering intensity, I, was plotted against the magnitude of the scattering vector, q [$q = 4\pi \sin(\theta/2)/\lambda$ with θ as the scattering angle and λ as the wavelength of incident beam]. At 30 °C, the SANS profile of the blend with 1 vol % of the copolymer (we call this blend B01) exhibited a scattering peak at $q = 0.038$ nm^{-1}, indicating the formation of a periodic structure with a charac-

[†] University of California, Berkeley.
[‡] Othmer-Jacobs Department of Chemical & Biological Engineering, Polytechnic University.
[§] National Institute of Standards and Technology.
[||] University of Maryland.
[⊥] Department of Chemical and Biological Sciences, Polytechnic University.
[#] Environmental and Energy Technologies Division, Lawrence Berkeley National Laboratory.
[×] Materials Sciences Division, Lawrence Berkeley National Laboratory.

10.1021/ma701922y CCC: $40.75
Published on Web 12/15/2007

Table 1. Characterization of Polymers in Blend B01[a]

component	name	M_w (kg/mol)	N	PDI	ρ (g/mL)	% 1,2-addition	n_D	φ
A	dPB89(24)	25.3	464	1.01	0.9070	90.4	2.79	0.488
B	PIB(24)	24.0	437	1.05	0.9131	NA	NA	0.502
A−C	hPBPB(240−192)	240−192	4614−3712	1.06	0.8629	86.5−61.5	NA	0.010

[a] M_w is the weight-averaged molecular weight, N is the number of reference volume units per chain based on a reference volume of 0.1 nm^3, PDI = $M_w/M_n$where M_n is the number-averaged molecular weight, ρ is the average density, n_D is the number of deuterium atoms per C_4 repeat unit, and φ is the volume fraction of each component.

teristic length scale $d = 2\pi/q = 160$ nm. In addition, the shape of the scattering peak was consistent with the well-established Teubner−Strey (T−S) scattering profile which is taken as a signature of the microemulsion phase.[17,22,33] Furthermore, the sample was perfectly clear when viewed either by the naked eye or in an optical microscope. When this blend was heated to 50 °C, the scattering peak could no longer be seen in the SANS data, but the scattering intensity obtained in the accessible q regime was consistent with the T−S equation.[31] This suggests that this blend may form a microemulsion with a length scale that is beyond the resolution limit of SANS. The purpose of this paper is to clarify the structure of the blend B01 using USANS and optical microscopy.

Ultra-small-angle scattering techniques (USAS, which includes both neutron and X-ray scattering) are rapidly emerging as powerful characterization tools for a wide variety of systems including polymer melts,[14,34−36] colloidal suspensions,[37−41] polymer solutions,[42,43] and gels.[44,45] A review of USAS studies was recently compiled by Bhatia.[46] In a majority of previous studies, a power law decay of the scattering intensity with increasing q was observed, indicating the absence of a well-defined length scale within the USAS range. For example, in the case of colloidal suspensions, the exponents of power law fits through the USAS profiles were used to determine the fractal dimensions of aggregates.[39] Many studies with polymer blends in the USAS range yield similar power law (or flat) scattering profiles.[14,35,42] Peaks that have been seen in USAS studies are often located at the upper end of the q range, where there is overlap with conventional small-angle X-ray and neutron scattering. For example, Koga et al. have reported a very prominent ultra-small-angle X-ray scattering (USAXS) peak in a polystyrene-*block*-polyisoprene system, but the peak was accessible by SAXS.[36] Broad USAXS peaks in the low-q limit were reported by Myers et al., who studied the morphology of polystyrene-*block*-polybutadiene.[34] However, reasons for the observed USAXS peak have not yet been fully established, and such peaks have not been observed in other studies of block copolymers.[14,36,42] In a previous study,[14] our group demonstrated the presence of a broad USANS shoulder in a multicomponent polymeric A/B/A−C microemulsion. It is interesting to note that none of the previous USAS studies[14,34−40,42−46] have presented evidence for the existence of micron-length scale periodic structures with well-defined scattering peaks. One of the goals of the present paper is to demonstrate the existence of such systems.

Experimental Section

Details concerning the synthesis and characterization of the polymers used in this study are described in ref 25. The homopolymers were dPB89(24), a saturated polybutadiene with 89% 1,2-addition (nominal value), and polyisobutylene, PIB(24). The numbers in parentheses refer to the molecular weight of the polymer molecules in kg/mol, and we refer to dPB89(24) as homopolymer A and PIB(24) as homopolymer B. The A−C copolymer, hPBPB-(240−192), is comprised of saturated polybutadiene blocks with 90% 1,2-addition and 62% 1,2 addition. Both A and A−C were synthesized by anionic polymerization of butadiene followed by saturation of the C=C bonds with either hydrogen or deuterium (labeled "h" or "d", respectively). The B homopolymer was synthesized by cationic polymerization. The characteristics of the polymers used in this study—density, weight-averaged molecular weight, polydispersity index, and % 1,2-addition for polybutadiene polymers—are summarized in Table 1. To create blend B01, the volume fraction ratio of the homopolymers, φ_A/φ_B, was set at 0.972, which is the value for a critical binary blend of A and B homopolymers based on the Flory−Huggins theory. The volume fraction of the A−C copolymer was 0.01. The components were dissolved in hexane followed by precipitation in a 50/50 mixture of methanol and acetone. The precipitant was placed on a 1 mm thick quartz disk inside a 1 mm thick spacer with an inner diameter of 8 mm. The sample was dried in a vacuum oven at 90 °C for 2 days to ensure complete removal of the solvent. A second quartz disk was pressed over the sample then the sample was annealed at 90 °C again for 10 min.

USANS measurements were conducted at the thermal neutron port BT5 at the National Institute of Standards and Technology (NIST) in Gaitherburg, MD. Details regarding instrumentation and data analysis are given in refs 47 and 48. The instrument consists of a Bonse-Hart type perfect-crystal diffractometer, equipped with triple bounce channel-cut perfect Si (220) crystals as the monochromator and the analyzer. The wavelength of the incident neutron beam, λ, was 0.238 nm, and the sample aperture diameter was 8 mm. A temperature-controlled sample stage is located between the monochromator and analyzer. The sample was annealed at the temperature of interest for 1−5 h in an effort to equilibrate the sample. Low-q scattering data obtained during annealing were invariably in good agreement with reported scattering data, suggesting that there was little change in morphology on the 1−5 h time scale. Larger equilibration times were not practical due to limited access to the USANS instrument. Data acquisition times ranged between 6 and 12 h, depending on scattering intensity and the q range of interest. The 1-dimensional raw scattering data were collected at discrete angular steps. These data were converted to absolute intensity (cm^{-1}) by correcting for sample transmission and background scattering using a data reduction program provided at NIST to give the USANS intensity, I, vs scattering vector, q.[48] The program provides a means for correcting for slit-smearing effects using the Lake method.[49] The reduction program was only run over the q range where the scattering signal was well above the background.

A Leica DM LP light microscope equipped with a CCD camera (Leica DC camera) and a temperature-controlled sample stage (Leica LMW) was used to study the morphology of the blend on time scales longer than 5 h. Images were taken in transmission mode at a magnification of 500× and were analyzed by local two-dimensional Fourier analysis as described in the next section.

The identification of any commercial product or trade name does not imply endorsement or recommendation by the National Institute of Standards and Technology.

Results and Discussion

Figure 1 compares the SANS results from ref 31 and the USANS results on blend B01 at 30 °C. Broad scattering peaks in the vicinity of $q = 0.035$ nm^{-1} are seen in both SANS and USANS. The USANS peak is located near the high-q limit of

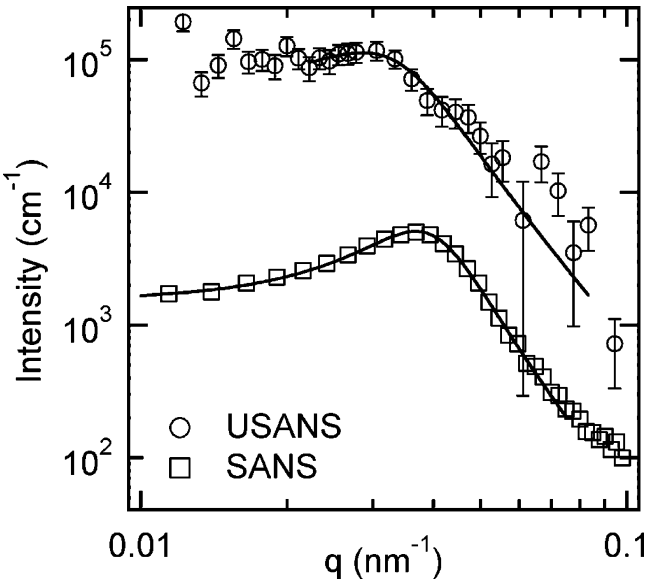

Figure 1. SANS (□) and USANS (○) data for blend B01 at 30 °C. The solid curves through the data are the Teubner−Strey fits.

the instrument. This leads to significantly larger error bars for the USANS data. The data were analyzed using the Teubner−Strey (T−S) equation, which is an established scattering signature of microemulsions:[33]

$$I(q) = \frac{1}{a + bq^2 + cq^4} \tag{1}$$

where a, b, and c are fitting parameters. The solid curves in Figure 1 are the least-squares fit of eq 1 through the data with a, b, and c as adjustable constants. The fitting constants can be used to determine the periodic domain spacing (d) and the correlation length (ξ) by

$$d = 2\pi\left[\frac{1}{2}\left(\frac{a}{c}\right)^{1/2} - \frac{1}{4}\left(\frac{b}{c}\right)\right]^{-1/2} \tag{2}$$

$$\xi = \left[\frac{1}{2}\left(\frac{a}{c}\right)^{1/2} + \frac{1}{4}\left(\frac{b}{c}\right)\right]^{-1/2} \tag{3}$$

The domain spacing calculated from the T−S fits of the SANS and USANS data are 160 and 200 nm, respectively. This length scale is much larger than the radii of gyrations (R_g) of the A, B, and A−C polymers, which are 4.1, 4.9, and 30.9 nm respectively. The value of ξ obtained from SANS and USANS are 90 and 80 nm, respectively. Considering the differences in instrumentation, the agreement between the SANS and USANS results is reasonable. We are not sure of the reason for the apparent vertical shift of the USANS data relative to the SANS data. However, such differences have been reported in previous studies where both SANS and USANS instruments were used to study the same system.[48] In ref 48, the observed vertical shift of the USANS data was attributed to slit smearing effects. In any case, the USANS experiment provides a self-consistent set of data, and the absolute intensity does not contribute to the T−S derived values. We attribute the differences in the domain spacings obtained by SANS and USANS to resolution differences between the instruments combined with the width of the microemulsion peak (Figure 1). USANS profiles obtained from B01 as a function of increasing temperature are shown in Figure 2. A broad but clearly defined scattering peak is evident at all of the temperatures studied. The peaks were consistent with the T−S equation (solid curves in Figure 2), indicating the presence

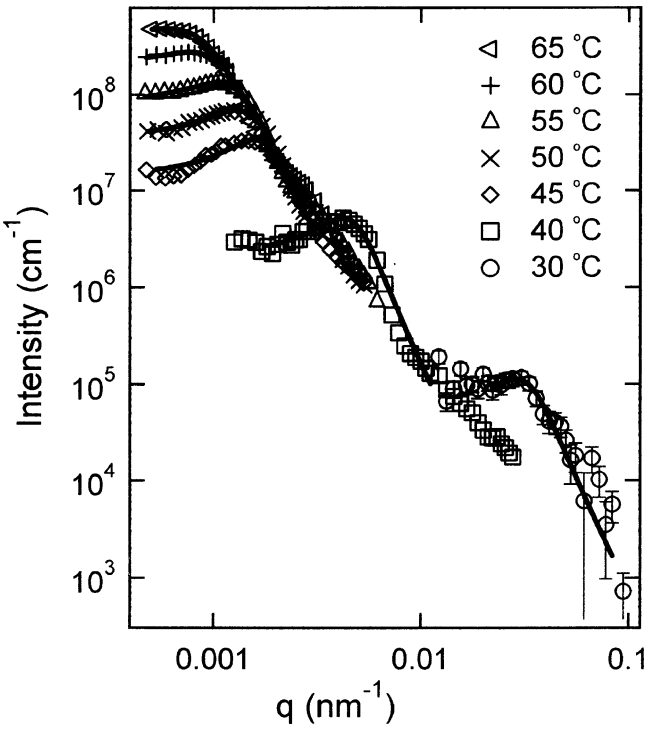

Figure 2. USANS profiles (not vertically shifted) for blend B01 as a function of increasing temperature. The solid curves are Teubner−Strey fits.

Table 2. Teubner−Strey Fitting Parameters

T (°C)	a (cm)	b (cm nm^2)	c (cm nm^4)	ξ (μm)	d (μm)
30	1.87×10^{-5}	−0.0247	15.4	0.08	0.20
40	4.67×10^{-7}	−0.0308	871.2	0.61	1.39
45	5.92×10^{-8}	−0.0243	5071.2	1.40	3.68
50	2.63×10^{-8}	−0.0142	4299.8	1.56	4.37
55	1.23×10^{-8}	−0.00847	3847.0	1.70	5.23
60	4.88×10^{-9}	−0.00421	3607.6	1.86	6.73
65	2.52×10^{-9}	−0.00257	3741.0	2.05	8.24

of a microemulsion-like structure. As the temperature is increased from 30 to 65 °C, d increases from 0.2 to 8.2 μm. The scattering intensity increased by 5 orders of magnitude in this temperature window. No evidence of macrophase separation is seen in any of the USANS profiles, and the sample remained optically clear throughout the experiment. The formation of periodic structures that are 2 orders of magnitude larger than the largest molecule in the system and 3 orders of magnitude larger than the molecules that make up most of the sample is noteworthy.

We conducted a second USANS run on B01 (several weeks after the first run) to confirm our conclusions about phase behavior. The temperature range of the second run was 30−75 °C (10 °C higher than the first run). The scattering profiles from both runs were qualitatively similar. The results of fits of the USANS profiles to the T−S equation are shown in Figure 3. In parts a and b of Figure 3, we show the domain spacing, d, and correlation length, ξ, respectively, obtained from both runs. Both d and ξ increase with increasing temperature. The agreement between the d values obtained from the two runs is significantly better than that of ξ, indicating that the correlation lengths of the delicate periodic structures formed in blend B01 are more sensitive to exact thermal history than the domain spacing. In equilibrated microemulsions, both d and ξ are governed by thermodynamics. In the case of lamellar phases, d is determined by thermodynamics while ξ is determined by processing and thermal history. The data in Figure 3 suggest that the microemulsion-like phase obtained at temperatures

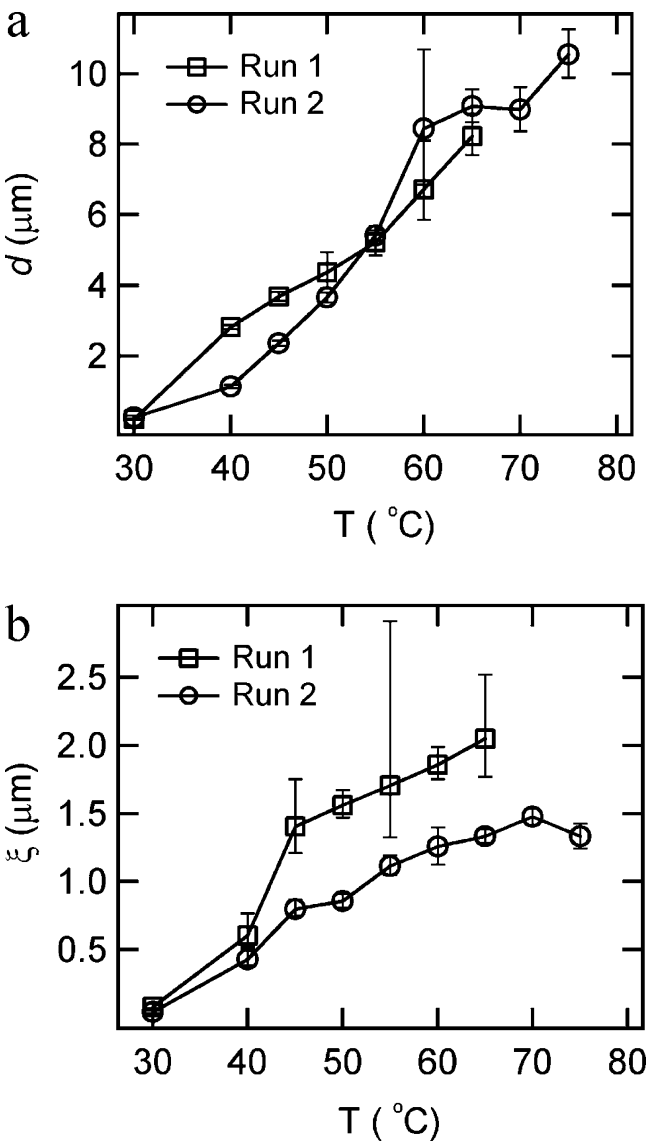

Figure 3. Temperature dependence of (a) d and (b) ξ for two separate runs on blend B01.

greater than or equal to 40 °C may not be at thermodynamic equilibrium.

Contrary to the first run, the sample became slightly cloudy at the end of the second run. However, after a few weeks at room temperature the sample became clear, suggesting that the large periodic structures formed at 75 °C relaxed spontaneously to give the microemulsion phase at room temperature. These observations indicate that the microemulsion obtained at 30 °C is thermodynamically stable, but equilibration times required for obtaining the microemulsion after heating the sample to 75 °C may be as large as 672 h (4 weeks).

In most of our USANS experiments, we studied the structure of the sample as a function of increasing temperature. In a few cases, we decreased the temperature of the blend. An example of results obtained from such experiments is shown in Figure 4, where we show $I(q)$ obtained from decreasing the temperature from 35 to 30 °C. We waited for 3.5 h before beginning data acquisition at 30 °C. If the phase obtained from B01 was indeed a microemulsion at both 30 and 35 °C and if equilibration occurred on experimentally accessible time scales, then we should have observed an increase in q_{peak}. Instead, we found no change in q_{peak} (Figure 4). We have established in Figure 1 that the equilibrium phase at 30 °C is a microemulsion. The lack of change in q_{peak} upon cooling indicates that the relaxation

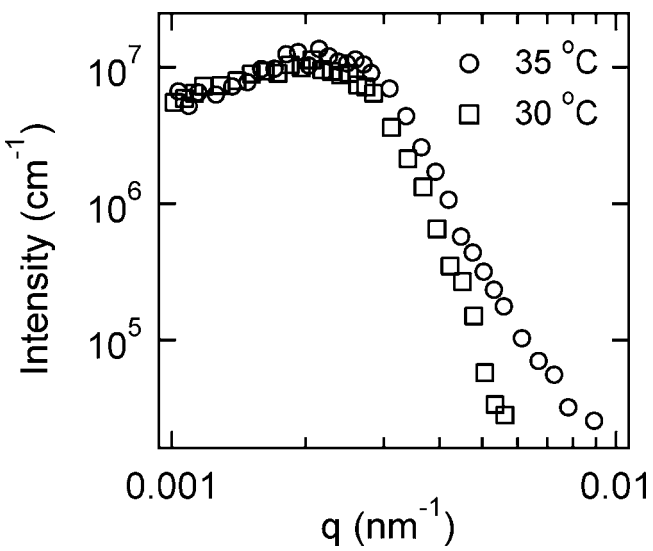

Figure 4. USANS data for blend B01 after decreasing temperature from 35 (○) to 30 °C (□).

of structures from 35 to 30 °C occurs on a time scale that is much larger than 3.5 h. We do, however, observe a decrease in the high q scattering intensity at 30 °C in Figure 4. This indicates that decreasing the temperature from 35 to 30 °C results in dissolution of the small length scale structures obtained at 35 °C on experimental time scales. On the other hand, the large length scale structures stay intact on the 3−4 h time scale. It is clear that long time scale studies are necessary to determine whether the microemulsions obtained in our blend are stable or metastable.

We also studied the morphology of B01 by optical microscopy. This approach is ideally suited for long time scale studies due to unlimited access to the instrument. The blend was completely clear at room temperature, and no structure was evident in the microscope. It was then heated to 43.5 ± 0.3 °C and annealed at that temperature for 8 days. (Our objective was to heat the sample to 40 °C to match the USANS experiments, but the analog dial on the Leica LMW temperature controller was difficult to fine-tune.) On the basis of the USANS data, we expected to obtain a microemulsion with a characteristic length scale of 1.4−3.9 μm (Figure 3a). The T−S equation applies equally well to both droplet and bicontinuous microemulsions. Since both kinds of microemulsions have been reported in A/B/A−C systems,[14] we were not sure of the morphology that we would see in the optical microscope. After 7 h of annealing, structures similar to a bicontinuous microemulsion became visible in the microscope. Selected micrographs obtained after annealing times of 7, 21, 96, and 193 h are shown in Figure 5a−d, respectively. The structures seen at 7, 21, and 96 h are similar to electron micrographs of bicontinuous microemulsions,[3,14] except for the fact that the length scales are in the 1−5 μm range. At extremely large annealing times of 193 h (8 days), we found streaklike microphases oriented along a particular direction, as shown in Figure 5d. We suspect that our sample stage may not have been perfectly horizontal, causing the sample to creep slowly over long times.

Two-dimensional Fourier analysis was used to obtain the periodic length scale, which we refer to as d for simplicity, from the optical micrographs. To perform the analysis, each image was divided into overlapping 512 × 512 pixels square boxes with centers separated by 30 pixels. 2D Fourier transforms (FT) were computed for each box and stored as a 512 × 512 array. Azimuthally symmetric FT images with peaks near the center of the FT image indicated the presence of the randomly oriented

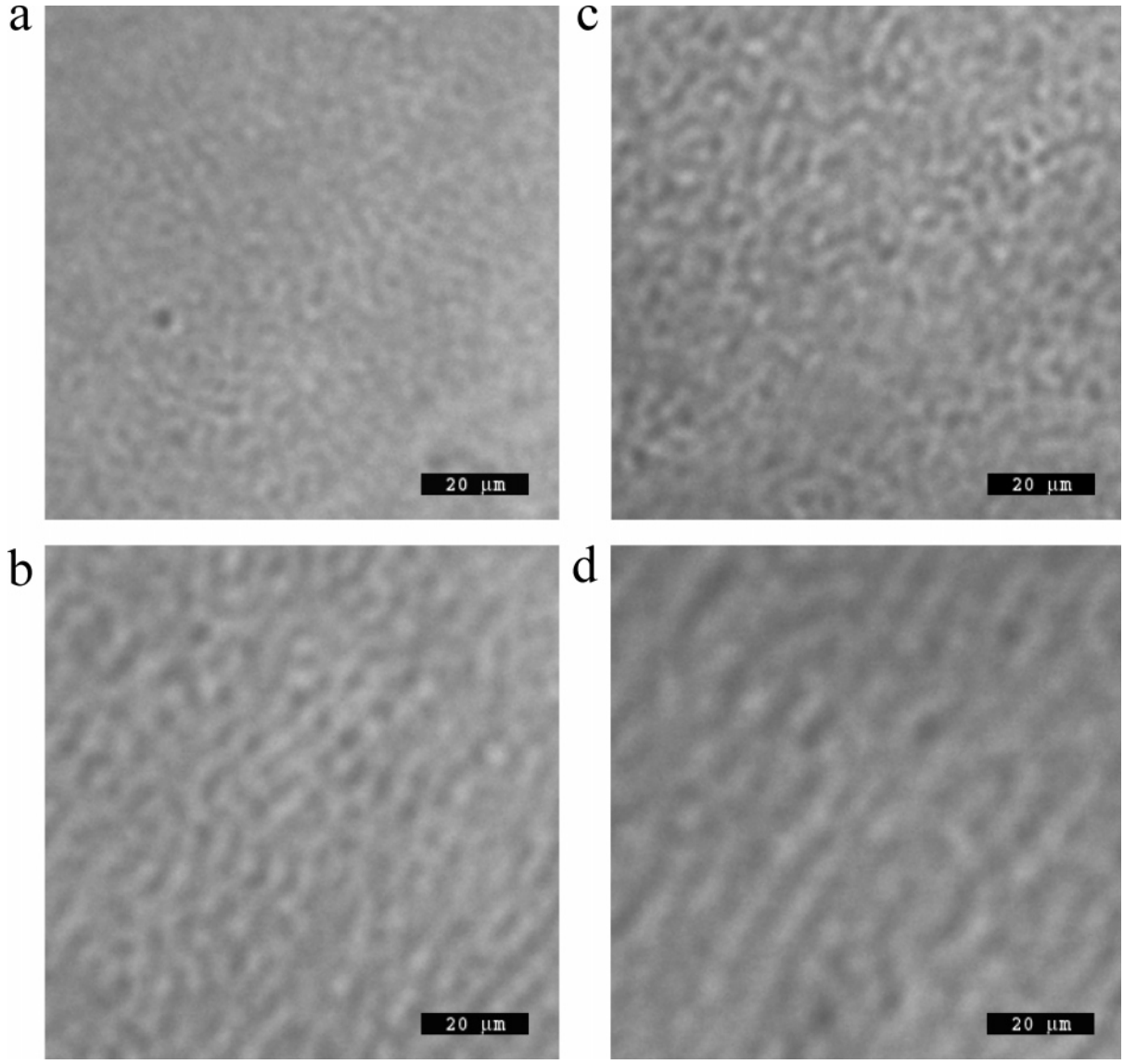

Figure 5. Optical micrographs of blend B01 at 43.5 ± 0.3 °C after (a) 7, (b) 21, (c) 96, and (d) 193 h.

periodic structure. Typical results are shown in Figure 6a, where the FT image of a box obtained at $t = 21$ h is shown. This image is a central cropped 160 × 160 pixel array from the original 512 × 512 FT array to better illustrate the data in the vicinity of the peak. To quantify the information in the FT images, we defined r to be the distance from a given pixel to the central one, in unit of pixels, and set $[r_j] = [3, 6, 9, ...]$. Values of the set $[A_j]$, the FT amplitude corresponding to the set $[r_j]$, were obtained by averaging the FT intensity within $r_j - 1.5 \leq r < r_j + 1.5$. The characteristic length scale of the periodic structure in each box, r^*, was determined by a least-squares fit of the $[A_j]$ vs $[r_j]$ data to the following functional form:

$$A(r) = C_1 \exp\left[\frac{-(r - r^*)^2}{w_1^2}\right] + C_2 \exp\left(\frac{-r}{w_2}\right) \qquad (4)$$

where r^*, C_1, C_2, w_1, and w_2 are fitting constants. Consequently, r is related to the scattering vector from USANS and r^* is similar to q_{peak}. In Figure 6b, we show the experimentally obtained $A(r)$ from the FT data shown in Figure 6a (circles). The solid curve through the data represents the least-squares fit of eq 4 through the data. Also shown in Figure 6b are the individual contributions of the peaked and decaying portions of $A(r)$ (the first and second terms on the right-hand side of eq 4, respectively). The measured d-spacing of a box is given by $512/r^*$ in units of pixels or $69.9/r^*$ in units of microns. The d-spacing of each image was obtained by averaging the measured d-spacing over all the overlapping boxes. Our analysis ignores the effect of defocusing and smearing of the optical image on the d-spacing.

The time dependence of d values obtained from the optical micrographs is shown in Figure 7. It is evident that the value of d increases slowly over a time scale of 100 h and approaches 4.3 μm at large times. Also shown in Figure 7 is the value of d obtained at early times by USANS at 40 and 45 °C. It is clear that the length scales of the bicontinuous microemulsion phase seen in the optical micrographs are consistent with the length scales obtained by USANS in the vicinity of the annealing temperature of 43 °C. It is not clear whether the slow increase in the optically determined d, seen in Figure 7, is due to temperature fluctuations or extremely slow approach toward equilibrium. We repeated the optical microscopy experiments at temperatures in the vicinity of 40 °C several times and got results that are similar to those reported in Figures 5 and 6. In no case did we see evidence of macrophase separation on experimental time scales. These results suggest that microemulsions with periodic length scales between 2 and 4.5 μm are obtained at equilibrium at temperatures between 40 and 45 °C.

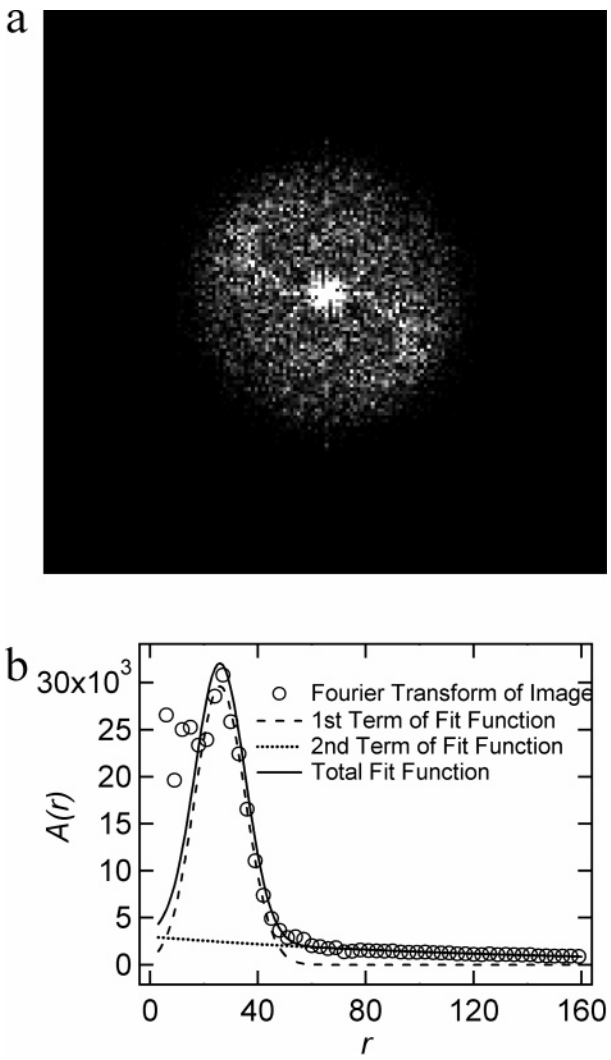

Figure 6. (a) Fourier transform of optical microscope image at $t =$ 21 h, cropped down from the original 512 × 512 array to focus on the central 160 × 160 array. (b) The FT was plotted as A_j vs r_j (○) and was fit to eq 4 (solid curve). The individual contributions from the first (dashed curve) and second (dotted curve) terms in eq 4 are also shown.

We repeated the optical microscopy experiment at 35 °C and were unable to detect any structures in the optical microscope, even after annealing for 193 h. On the other hand, annealing the sample at 60 ± 3 °C resulted in structures that were qualitatively similar to those seen in Figure 5 for the first 3 days. However, macrophase separation was seen on the fourth day. On the basis of these observations, we conclude that sample B01 forms a microemulsion phase at temperatures between room temperature and 45 °C and phase-separated structures at temperatures ≥60 °C. The microemulsion-like phases observed by USANS at temperatures ≥60 °C (Figure 3) are thus metastable. Predictions using multicomponent self-consistent-field theory (SCFT)[25] indicate the presence of large structures at equilibrium (around 0.85 μm at 45 °C). Determining the stability of the microemulsion-like phases at temperatures between 45 and 60 °C would probably require observing the sample at time scales much larger than 1 week and were thus not attempted.

Conclusions

Our objective was to determine the morphology and thermodynamic properties of a multicomponent polymer mixture

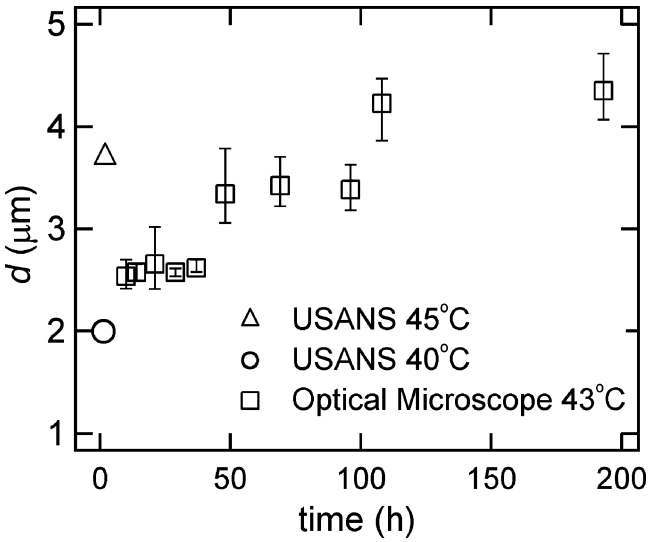

Figure 7. Average *d*-spacing of bicontinuous microemulsion-like structures in blend B01 at 43.5 °C as calculated from optical micrograph images (□) as a function of time. The points at 2 h are the *d*-spacing calculated from Teubner−Strey fits of the USANS data at 45 (△) and 40 °C (○).

composed of a critical blend of two homopolymers, dPB89-(24) and PIB(24), with a hPBPB(240−192) diblock copolymer. The volume fraction of the hPBPB(240−192) was 0.01. This blend forms a thermodynamically stable microemulsion at temperatures between 30 and 45 °C and undergoes macrophase separation at 60 °C. At temperatures between 35 and 60 °C, USANS studies showed the existence of clearly defined scattering peaks that were consistent with the Teubner−Strey equation for scattering from microemulsions. The characteristic length scale of the microemulsion-like structure formed at these temperatures ranged from 0.47 to 8.4 μm. To our knowledge, this is the only study on polymer blends where well-defined peaks are seen in USAS. Our USANS experiments were restricted to annealing times that were less than 5 h, and the microemulsion-like phase appeared stable on those time scales. More extensive annealing studies, using an optical microscope, revealed the presence of a bicontinuous microemulsion in the 40−45 °C temperature window that was stable for 1 week. These studies enabled the determination of the temperature above which our blend undergoes macrophase separation (60 °C). This work demonstrates that determining the thermodynamic properties of blends containing small concentrations of block copolymers near the macrophase separation temperature is difficult due to extremely slow evolution of the structure. It is important to note that the components of the blend are well above their glass transition temperatures (the glass transition temperatures of saturated polybutadiene and polyisobutylene are −30 and −60 °C, respectively). In addition, the molecular weights of the major components of the blends are relatively low (25 kg/mol). The slow evolution of structure between 40 and 60 °C cannot be attributed to slow molecular motion and must therefore be due to extremely small thermodynamic driving forces. Further work to elucidate the kinetics of microphase and macrophase separation in the limit of very low block copolymer concentration seems warranted.

Acknowledgment. This material is based upon work supported by the National Science Foundation under Grants CBET-0625785 and DMR-0514422 and a National Science Foundation Graduate Research Fellowship. We acknowledge the support of the National Institute of Standards and Technology, U.S.

Department of Commerce, in providing the neutron research facilities used in this work. This work utilized facilities supported in part by the National Science Foundation under Agreement DMR-0454672.

References and Notes

(1) Leibler, L. *Makromol. Chem., Rapid Commun.* **1981**, *2*, 393−400.
(2) Broseta, D.; Fredrickson, G. H. *J. Chem. Phys.* **1990**, *93*, 2927−2938.
(3) Bates, F. S.; Maurer, W. W.; Lipic, P. M.; Hillmyer, M. A.; Almdal, K.; Mortensen, K.; Fredrickson, G. H.; Lodge, T. P. *Phys. Rev. Lett.* **1997**, *79*, 849−852.
(4) Bates, F. S.; Maurer, W.; Lodge, T. P.; Schulz, M. F.; Matsen, M. W.; Almdal, K.; Mortensen, K. *Phys. Rev. Lett.* **1995**, *75*, 4429−4432.
(5) Adedeji, A.; Hudson, S. D.; Jamieson, A. M. *Macromolecules* **1996**, *29*, 2449−2456.
(6) Adedeji, A.; Hudson, S. D.; Jamieson, A. M. *Polymer* **1997**, *38*, 737−741.
(7) Xu, Z.; Jandt, K. D.; Kramer, E. J.; Edgecombe, B. D.; Frechet, J. M. J. *J. Polym. Sci., Part B: Polym. Phys.* **1995**, *33*, 2351−2357.
(8) Shull, K. R.; Kellock, A. J.; Deline, V. R.; Macdonald, S. A. *J. Chem. Phys.* **1992**, *97*, 2095−2104.
(9) Braun, H.; Rudolf, B.; Cantow, H. J. *Polym. Bull. (Berlin)* **1994**, *32*, 241−248.
(10) Ravikumar, H. B.; Ranganathaiah, C.; Kumaraswamy, G. N.; Urs, M. V. D.; Jagannath, J. H.; Bawa, A. S.; Thomas, S. *J. Appl. Polym. Sci.* **2006**, *100*, 740−747.
(11) Tseng, F. P.; Tseng, C. R.; Chang, F. C.; Lin, J. J.; Cheng, I. J. *J. Polym. Res.* **2005**, *12*, 439−447.
(12) Jannasch, P.; Hassander, H.; Wesslen, B. *J. Polym. Sci., Part B: Polym. Phys.* **1996**, *34*, 1289−1299.
(13) Wang, Z. G.; Safran, S. A. *J. Chem. Phys.* **1991**, *94*, 679−687.
(14) Lee, J. H.; Ruegg, M. L.; Balsara, N. P.; Zhu, Y. Q.; Gido, S. P.; Krishnamoorti, R.; Kim, M. H. *Macromolecules* **2003**, *36*, 6537−6548.
(15) Janert, P. K.; Schick, M. *Macromolecules* **1998**, *31*, 1109−1113.
(16) Stepanek, P.; Morkved, T. L.; Bates, F. S.; Lodge, T. P.; Almdal, K. *Macromol. Symp.* **2000**, *149*, 107−112.
(17) Washburn, N. R.; Lodge, T. P.; Bates, F. S. *J. Phys. Chem. B* **2000**, *104*, 6987−6997.
(18) Hillmyer, M. A.; Maurer, W. W.; Lodge, T. P.; Bates, F. S.; Almdal, K. *J. Phys. Chem. B* **1999**, *103*, 4814−4824.
(19) Kahlweit, M.; Strey, R. *Angew. Chem., Int. Ed. Engl.* **1985**, *24*, 654−668.
(20) Kahlweit, M.; Strey, R.; Firman, P.; Haase, D. *Langmuir* **1985**, *1*, 281−288.
(21) Kahlweit, M.; Strey, R.; Haase, D.; Firman, P. *Langmuir* **1988**, *4*, 785−790.
(22) Strey, R. *Colloid Polym. Sci.* **1994**, *272*, 1005−1019.
(23) Chen, S. H.; Choi, S. *Supramol. Sci.* **1998**, *5*, 197−206.
(24) Reynolds, B. J.; Ruegg, M. L.; Balsara, N. P.; Radke, C. J. *Langmuir* **2006**, *22*, 9201−9207.
(25) Reynolds, B. J.; Ruegg, M. L.; Balsara, N. P.; Radke, C. J.; Shaffer, T. D.; Lin, M. Y.; Shull, K. R.; Lohse, D. J. *Macromolecules* **2004**, *37*, 7401−7417.
(26) Reynolds, B. J.; Ruegg, M. L.; Mates, T. E.; Radke, C. J.; Balsara, N. P. *Macromolecules* **2005**, *38*, 3872−3882.
(27) Reynolds, B. J.; Ruegg, M. L.; Mates, T. E.; Radke, C. J.; Balsara, N. P. *Langmuir* **2006**, *22*, 9192−9200.
(28) Ruegg, M. L.; Newstein, M. C.; Balsara, N. P.; Reynolds, B. J. *Macromolecules* **2004**, *37*, 1960−1968.
(29) Ruegg, M. L.; Patel, A. J.; Narayanan, S.; Sandy, A. R.; Mochrie, S. G. J.; Watanabe, H.; Balsara, N. P. *Macromolecules* **2006**, *39*, 8822−8831.
(30) Ruegg, M. L.; Reynolds, B. J.; Lin, M. Y.; Lohse, D. J.; Balsara, N. P. *Macromolecules* **2006**, *39*, 1125−1134.
(31) Ruegg, M. L.; Reynolds, B. J.; Lin, M. Y.; Lohse, D. J.; Balsara, N. P. *Macromolecules* **2007**, *40*, 1207−1217.
(32) Ruegg, M. L.; Reynolds, B. J.; Lin, M. Y.; Lohse, D. J.; Krishnamoorti, R.; Balsara, N. P. *Macromolecules* **2007**, *40*, 355−365.
(33) Teubner, M.; Strey, R. *J. Chem. Phys.* **1987**, *87*, 3195−3200.
(34) Myers, R. T.; Cohen, R. E.; Bellare, A. *Macromolecules* **1999**, *32*, 2706−2711.
(35) Agamalian, M.; Alamo, R. G.; Kim, M. H.; Londono, J. D.; Mandelkern, L.; Wignall, G. D. *Macromolecules* **1999**, *32*, 3093−3096.
(36) Koga, T.; Koga, T.; Hashimoto, T. *J. Chem. Phys.* **1999**, *110*, 11076−11086.
(37) Pontoni, D.; Narayanan, T. *J. Appl. Crystallogr.* **2003**, *36*, 787−790.
(38) Shah, S. A.; Chen, Y. L.; Ramakrishnan, S.; Schweizer, K. S.; Zukoski, C. F. *J. Phys.: Condens. Matter* **2003**, *15*, 4751−4778.
(39) Muzny, C. D.; Butler, B. D.; Hanley, H. J. M.; Agamalian, M. *J. Phys.: Condens. Matter* **1999**, *11*, L295−L298.
(40) Bhatia, S.; Barker, J.; Mourchid, A. *Langmuir* **2003**, *19*, 532−535.
(41) Gabriel, J.-C. P.; Camerel, F.; Lemaire, B. J.; Desvaux, H.; Davidson, P.; Batail, P. *Nature (London)* **2001**, *413*, 504−508.
(42) Crichton, M. A.; Bhatia, S. R. *Langmuir* **2005**, *21*, 10028−10031.
(43) Won, Y. Y.; Davis, H. T.; Bates, F. S.; Agamalian, M.; Wignall, G. D. *J. Phys. Chem. B* **2000**, *104*, 9054−9054.
(44) Takeshita, H.; Kanaya, T.; Nishida, H.; Kaji, K. *Macromolecules* **1999**, *32*, 7815−7819.
(45) Takeshita, H.; Kanaya, T.; Nishida, K.; Kaji, K.; Takahashi, T.; Hashimoto, M. *Phys. Rev. E* **2000**, *61*, 2125−2128.
(46) Bhatia, S. R. *Curr. Opin. Colloid Interface Sci.* **2005**, *9*, 404−411.
(47) Barker, J. G.; Glinka, C. J.; Moyer, J. J.; Kim, M. H.; Drews, A. R.; Agamalian, M. *J. Appl. Crystallogr.* **2005**, *38*, 1004−1011.
(48) Kline, S. R. *J. Appl. Crystallogr.* **2006**, *39*, 895−900.
(49) Lake, J. A. *Acta Crystallogr.* **1967**, *23*, 191−194.

MA701922Y